N,N′-diisopropylthiourea and N,N′-dicyclohexylthiourea zinc(II) complexes as precursors for the synthesis of ZnS nanoparticles

N. Moloto[a,b], N. Revaprasadu[a*], M.J. Moloto[c], P. O'Brien[d*] and J. Raftery[d]

The single X-ray crystal structures of zinc (II) complexes of N,N′-diisopropylthiourea and N,N′-dicyclohexylthiourea were determined. These complexes, similar to other alkylthioureas, were found to be effective as precursors for the preparation of hexadecylamine-capped ZnS nanoparticles. The complexes are air-stable, easy to prepare and inexpensive. They pyrolyse cleanly to give high-quality ZnS nanoparticles, which show quantum confinement effects in their absorption spectra and close to band-edge emission. Their broad diffraction patterns are typical of nanosized particles while their transmission electron microscopy images showed agglomerates of needle-like platelet nanoparticles.
Key words: N,N′-diisopropylthiourea, N,N′-dicyclohexylthiourea, synthesis, ZnS nanoparticles, precursor

Introduction

The size-dependent optical properties of semiconducting metal chalcogenide nanoparticles have made them highly attractive for many technological applications. ZnS materials doped with various metal ions have been used as phosphors for electronic displays.[1] Nanostructured doped ZnS materials have attracted considerable attention because of their superior luminescent characteristics, compared to those of their bulk counterparts.[2–5] These unique properties have led to many applications, such as optical coatings, solid-state solar cell windows, electro-optic modulators, photoconductors, field-effect transistors, sensors and transductors, as well as light-emitting applications.[6] As efficient phosphors, ZnS particles have been widely implicated in flat-panel displays,[7] thin-film electroluminescent devices and infrared windows.[8] Nanosized ZnS and manganese-doped ZnS have been prepared by precipitation methods,[9] in structured media such as polymers and gel films,[10] and by using single-molecule precursors.[11]

Over the past few years, attention has focused on the research field of one-dimensional nanostructured materials, such as nanowires or nanorods, because of their fundamental importance and the wide range of their potential applications in nanodevices.[12] In order to obtain nanowires or nanorods of the desired materials, many methods have been used for the preparation of one-dimensional nanostructured materials, such as laser ablation,[13] template synthesis,[14–16] solution-based routes[17–19] and other methods.[20–23] The use of molecular precursors containing both the metal and chalcogenide, initially reported by Trindade and O'Brien,[24,25] have proven to be an efficient route to high-quality crystalline, monodispersed, semiconducting nanoparticles. The use of the cadmium alkylthiourea complexes as precursors for the synthesis of CdS have been previously reported by our group.[26,27] In the present study, we successfully synthesised zinc (II) complexes of N,N-diisopropylthiourea and N,N-dicyclohexylthiourea and report their single X-ray crystal structures. These complexes were then thermolysed in hexadecylamine (HDA) to give organically-capped ZnS nanoparticles.

[a]Department of Chemistry, University of Zululand, Private Bag X1001, KwaDlangezwa 3886, South Africa.
[b]Macromolecular Nanotechnology Research Group, National Centre for Nanostructured Materials, CSIR Materials Science and Manufacturing, P.O. Box 395, Pretoria 0001, South Africa.
[c]School of Chemistry, University of Witwatersrand, Private Bag 3, WITS 2050, South Africa.
[d]Department of Chemistry, The Manchester Materials Science Centre, The University of Manchester, Oxford Rd., Manchester, M13 9PL, U.K.
*Authors for correspondence
E-mail: nrevapra@pan.uzulu.ac.za / paul.obrien@manchester.ac.uk

Methods

Hexadecylamine and tri-n-octylphosphine (TOP) were purchased from Aldrich. Toluene and methanol were obtained from BDH. Toluene was stored over molecular sieves (40Å, BDH) before use. Zinc chloride, N,N′-diisopropylthiourea, N,N′-dicyclohexylthiourea and ethanol (analytical grade) were used, as purchased from Aldrich, to prepare the precursors.

Optical characterisation

A Perkin Elmer Lambda 20 UV-VIS spectrophotometer was used to perform the optical measurements; the samples were placed in silica cuvettes (1-cm path length), using toluene as a reference solvent. A Jobinyvon-spex-Fluorolog-3-Spectro fluorometer with a xenon lamp (150 W) and a 152 P photomultiplier tube as a detector were used to measure the photoluminescence of the particles. The samples were placed in quartz cuvettes (1-cm path length).

Electron microscopy

The transmission electron microscopy (TEM) and high-resolution transmission electron microscopy (HRTEM) images were obtained using a Philips CM 200 compustage electron microscope operated at 200 kV with an energy dispersive spectroscopy analyser. The samples were prepared by placing a drop of a dilute solution of sample in toluene on a copper grid (400 mesh, agar). The samples were allowed to dry completely at room temperature.

X-ray crystallography

The X-ray data were collected at 100 K on a Bruker Smart Apex CCD diffractometer, using Mo Kα radiation, from crystals mounted in a Hamilton Cryoloop. Data were reduced by SAINTPLUS. The structures were solved by direct methods using SHELXS-9719[28] (I) or SIR200420[29] (II) and refined anisotropically (non-hydrogen atoms) by full-matrix least-squares on F2 using SHELXL-9721.[30] The H atoms were calculated geometrically and refined with a riding model.

The X-ray diffraction patterns on the powdered samples were measured on Phillips X'Pert materials research diffractometer using secondary graphite monochromated Cu Kα radiation (λ = 1.54060 Å) at 40 kV 50 mA^{-1}. Samples were supported on glass slides. Measurements were taken using a glancing angle of

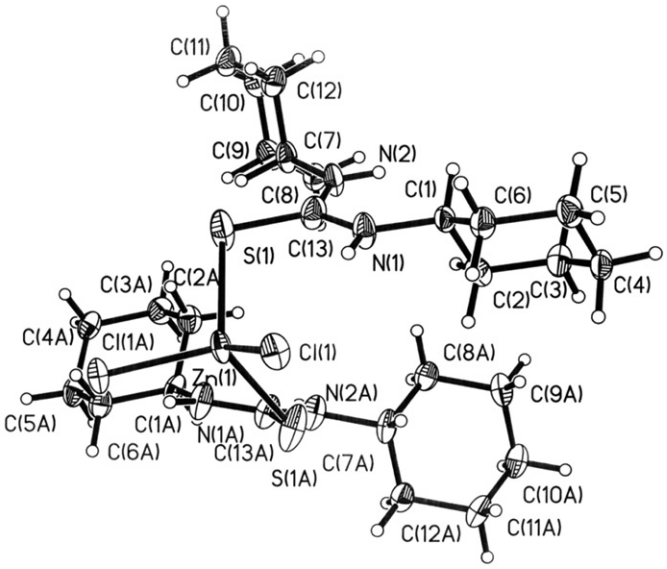

Fig. 1. Molecular structure of complex **I**, $[ZnCl_2((CS(NHC_6H_{11})_2)_2]$.

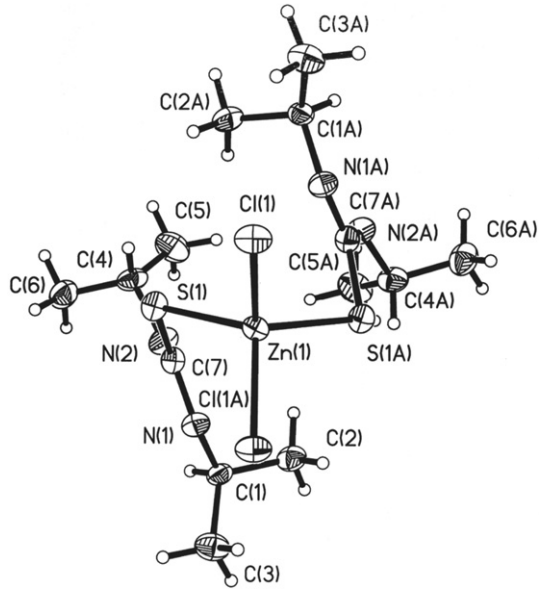

Fig. 2. Molecular structure of complex **II**, $[ZnCl_2((CS(NHC_3H_7)_2)_2]$.

incidence detector at an angle of 2°, for 2θ values over 20–60° in steps of 0.05° with a scan speed of 0.01° s^{-1}.

Elemental analysis

Elemental analysis is the determination of the percentage weights of carbon (C), hydrogen (H), nitrogen (N) and heteroatoms (X) (halogens, sulphur (S)) of a sample. The elemental analysis was performed on a CARLO ERBA elemental analyser for C, H, N and S. The sample was burned in excess oxygen and the combustion products were analysed by inductively-coupled mass spectrometry.

Fourier transform infrared (FTIR) and nuclear magnetic resonance spectroscopy

Infrared spectra were recorded on a FTIR Perkin Elmer paragon 1 000 spectrophotometer using nujol mull. Nuclear magnetic resonance (NMR) spectra were recorded on a Varian Associates Inova spectrometer (400 MHz and 300 MHz).

Synthesis of precursors

$[ZnCl_2(CS(NHC_6H_{11})_2)_2]$ (I). A hot solution of N,N′-dicyclohexylthiourea (1 g, 4.16 mmol) in ethanol (20 ml) was added to a heated solution of zinc chloride (0.28 g, 2.08 mmol) in ethanol (25 ml). The mixture was stirred and refluxed for 1 h. The colourless solution was filtered hot to remove any traces of unreacted materials and was left in an open beaker at room temperature. The colourless crystalline product was obtained after 24 h. The product was filtered, washed twice with ethanol and dried under vacuum. Yield 76.4%; m.p. 230.3–233.5°C. $C_{26}H_{48}N_4S_2Zn$: Anal. Calcd. C, 50.62; H, 7.79; N, 9.09; S, 10.38. Found: C, 50.70; H, 7.99; N, 9.04; S, 10.14. IR (nujol mull)/cm^{-1}: 3286(vs), 2931 (vs), 2854(m), 1558(vs), 1450(s), 1342(w), 1234(s), 1157(vw), 1095(w), 972(s), 894(m), 817(vw), 771(m). ^{1}H NMR (δ, $CdCl_3$) ppm: 4.10 (s, 3H, CH_3); 3.92 (s, 3H, CH_3). ^{13}C {^{1}H} NMR (δ, $CdCl_3$) ppm: 179.38 (s, CS); 31.22 (s, CH_3).

$[ZnCl_2(CS(NHC_3H_7)_2)_2]$ (II). A hot solution of N,N′-diisopropylthiourea (1 g, 6.25 mmol) in ethanol (20 ml) was added to a heated solution of zinc chloride (0.43 g, 3.13 mmol) in ethanol (25 ml). The mixture was stirred and refluxed for 1 h. The colourless solution was filtered hot to remove any traces of unreacted materials and was left in an open beaker at room temperature. A colourless needle-like crystalline product was obtained after 24 h. The product was filtered, washed twice with ethanol and dried under vacuum. Yield 62.7%; m.p. 192.1–193.8°C. $C_{14}H_{32}N_4S_2Zn$: Anal. Calcd. C, 36.81; H, 7.01; N, 12.27; S, 14.02. Found: C, 36.69; H, 7.06; N, 12.22; S, 13.73. IR (nujol mull)/cm^{-1}: 3271(vs), 2978(s), 1558(vs), 1450(s), 1388(sh), 1280(s), 1141(s), 956(m), 848(w). ^{1}H NMR (δ, $CdCl_3$) ppm: 2.15 (d, 2H, C_3H_7); 1.60 (s, 6H, C_3H_7), 7.22 (s, 2H, NH). ^{13}C {^{1}H} NMR (δ, $CdCl_3$) ppm: 179.38 (s, CS); 31.22 (s, CH_3).

Preparation of ZnS nanoparticles

In a typical experiment, $[ZnCl_2(SC(NHC_6H_{11})_2]$ (precursor I) (1 g) was dissolved in TOP (10–15 ml). This solution was then injected into 6.25 g of hot HDA at a temperature of 180°C. A subsequent decrease in temperature of 20–30°C was observed. The solution was allowed to stabilise at 180°C and heated for a further 60 min. The solution was then allowed to cool to about 70°C, and methanol was added to remove the excess HDA. The as-synthesised flocculent precipitate was separated by centrifugation and redispersed in toluene. The solvent was then removed by evaporation under reduced pressure to give HDA-capped ZnS nanoparticles. The particles were washed three times with methanol and redispersed in toluene. This same procedure was followed using precursor II, $ZnCl_2(CS(NHC_3H_7)_2)_2$ to prepare HDA-capped ZnS nanoparticles.

Results and discussion

Single X-ray structures

Both complexes were subjected to single crystal X-ray structural analysis, crystallised in methanol by slow evaporation at room temperature to give transparent cube-shaped crystals. They were stable in air and moisture with melting points of 192°C and 230°C, for complex **II** and **I**, respectively. The formulae of the resulting complexes were consistent with the molecular structures and other forms of analyses, such as microanalysis, infrared and NMR spectroscopy. Details of the crystal data and structure refinements are provided in Table 1. ORTEP diagrams of complexes **I** and **II** with the non-hydrogen atomic labelling scheme are shown in Figs 1 and 2, respectively. Selected bond lengths and angles are given in Tables 2 and 3. The structures were deposited at the CCDC with deposition numbers of 642408 and 642407, for complexes **I** and **II**, respectively.

Table 1. Crystal data and detailed structure refinement for complexes **I** and **II**.

Complex:	**I**	**II**
Empirical formula	$C_{26}H_{48}ZnCl_2N_4S_2$	$C_{14}H_{32}ZnCl_2N_4S_2$
Formula weight	617.07	456.83
Temperature	100(2) K	100(2) K
Wavelength	0.71073 Å	0.71073 Å
Crystal system	Monoclinic	Orthorhombic
Space group	C2/c	Pbcn
Unit cell dimensions	a = 11.2990(12) Å; α = 90° b = 14.6130(16) Å; β = 90.64° c = 19.223(2) Å; γ = 90°	a = 9.5010(8) Å; α = 90° b = 14.8110(12) Å; β = 90°. c = 15.6750(13) Å; γ = 90°
Volume	3173.8(6) Å^3	2205.8(3) Å^3
Z	4	4
Density (calculated)	1.291 mg m^{3}	1.376 mg m^{3}
Absorption coefficient	1.095 mm^{1}	1.549 mm^{1}
F(000)	1 312	960
Crystal size	0.20 × 0.18 × 0.12 mm^3	0.33 × 0.15 × 0.12 mm^3
θ range for data collection	2.12–28.28°	2.55–28.26°
Index ranges	–14 ≤ h ≤ 10, –19 ≤ k ≤ 18, –24 ≤ l ≤ 23	–12 ≤ h ≤ 7, –19 ≤ k ≤ 16, –20 ≤ l ≤ 20
Reflections collected	9 849	13 002
Independent reflections	3 706 [R(int) = 0.0489]	2 664 [R(int) = 0.0553]
Completeness to θ (24.98°)	93.7%	96.9%
Maximum and minimum transmission	0.8798 and 0.8108	0.8360 and 0.6290
Goodness-of-fit on F^2	0.982	1.058
Final R indices	R1 = 0.0533, wr2 = 0.1306	R1 = 0.0626, wr2 = 0.1734
R indices (all data)	R1 = 0.0835, wr2 = 0.1377	R1 = 0.0759, wr2 = 0.1792
Largest diff. peak and hole	0.963 and –0.499 e.Å^{3}	1.645 and –0.650 e.Å^{3}

Table 2. Selected bond distances (Å) and bond angles (°) for complex **I**.

Bond distances (Å)		Bond angles (°)	
Zn(1)–Cl(1)	2.2611(9)	Cl(1)–Zn(1)–S(1)	111.08(4)
Zn(1)–S(1)	2.3181(12)	S(1)–Zn(1)–S(1)1	115.53(7)
Zn(1)–Cl(1)1	2.2611(9)	Cl(1)–Zn(1)–S(1)1	101.17(4)
Zn(1)–S(1)1	2.3181(12)	Cl(1)1–Zn(1)–S(1)1	111.08(4)
S(1)–C(13)	1.719(4)	Cl(1)1–Zn(1)–S(1)	101.17(4)
N(2)–C(13)	1.335(5)	Cl(1)1–Zn(1)–Cl(1)	117.51(5)
N(1)–C(13)	1.333(5)		
N(2)–C(7)	1.475(5)		
N(1)–C(1)	1.472(4)		

Table 3. Selected bond distances (Å) and bond angles (°) for complex **II**.

Bond distances (Å)		Bond angles (°)	
Zn(1)–Cl(1)	2.2662(11)	Cl(1)–Zn(1)–S(1)	105.73(4)
Zn(1)–S(1)	2.3401(11)	S(1)–Zn(1)–S(1)1	111.33(6)
Zn(1)–Cl(1)1	2.2661(11)	Cl(1)–Zn(1)–S(1)1	110.74(4)
Zn(1)–S(1)1	2.3402(11)	Cl(1)1–Zn(1)–S(1)1	105.73(4)
S(1)–C(7)	1.714(5)	Cl(1)1–Zn(1)–S(1)	110.74(4)
N(1)–C(7)	1.344(6)	Cl(1)1–Zn(1)–Cl(1)	112.68(6)
N(2)–C(7)	1.326(6)		
N(2)–C(4)	1.481(6)		
N(1)–C(1)	1.501(6)		

Molecular description of complex **I**

The structure of complex **I**, $[ZnCl_2((CS(NHC_6H_{11})_2)_2]$ (Fig. 1), is based on a discrete monomeric molecule with the coordination polyhedra around the Zn(II) ion a distorted tetrahedral. The two N,N′-dicyclohexylthiourea ligands were sulphur-bonded to the metal atom with the two chloride ligands facing opposite to the two organic ligands. In this four-coordinate structure, molecular units are arranged so that one of the chloride ions (Cl(1)) and the zinc atom lie on a crystallographic three-fold axis which relates to the two thiourea ligands and the second chlorine atom (Cl(1)1). The average bond distances for Zn–Cl bonds are 2.261 Å and the Zn–S bonds gave an average value of 2.318 Å, which is slightly shorter than for the corresponding zinc complex **II** (Table 3). The S–C bond distances in the thiourea ligands are typically intermediate between a single and double bond character, which is 1.719 Å. The C–N bond distances range from an intermediate bond character of 1.475 Å to an almost double bond character of 1.333 Å. These slightly shorter bond distances could be influenced by the steric and electronic effects of the cyclohexyl groups. The lengths of the C–N and C–S bonds are intermediate between the values expected for single and double bonds, thus indicating that the canonical forms make a substantial contribution to the structure.

The two cyclohexyl rings on one thiourea ligand are planar and chair forms on the other. The S(1)–Zn(1)–Cl(1) and S(1)1–Zn(1)–Cl(1)1 bond angles are both 111.08°, and Cl(1)–Zn(1)–S(1)1 and S(1)–Zn(1)–Cl(1)1 bond angles are both 101.17°. The bond angles for two similar atoms bonded to the zinc atom, S(1)–Zn(1)–S(1)1 and Cl(1)1–Zn(1)–Cl(1), are slightly bigger at 115.53° and 117.51°, respectively. This is expected for the cyclohexyl group and these angles deviate from the regular tetrahedral value of 109.47°, which could be explained by the steric interaction between the cyclohexyl groups. The structural analysis of this complex is in agreement with the spectroscopic data obtained for this compound.

Molecular description of complex **II**

The structure of complex **II**, $[ZnCl_2(CS(NHC_3H_7)_2)_2]$ (Fig. 2), is based on a discrete monomeric molecule with the coordination polyhedra around the Zn(II) ion being that of a distorted tetrahedral. The two N,N′-diisopropylthiourea ligands were sulphur-bonded to the metal atom with the two chloride ligands completing the geometry. In this four-coordinate structure, molecular units are arranged so that one of the chloride ions (Cl(1)) and the metal atom lie on a crystallographic three-fold axis which relates to the two thiourea ligands and the second chlorine atom (Cl(1)1). The average bond distances for Zn–Cl bonds are 2.266 Å and 2.340 Å for Zn–S bonds. The S–C bond

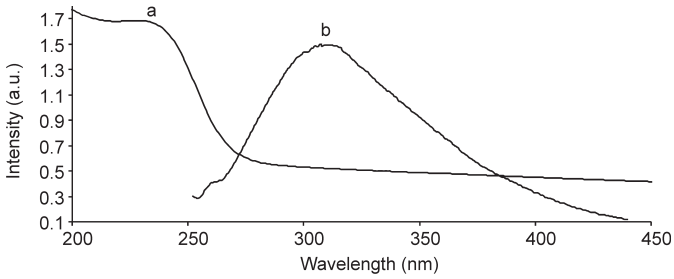

Fig. 3. Absorption (a) and emission (b) spectra of HDA-capped ZnS nanoparticles prepared from precursor I at 180°C for 60 min.

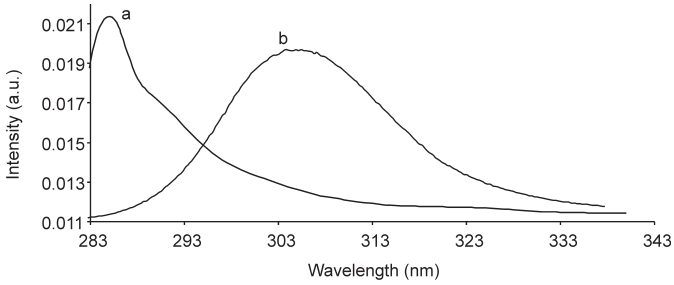

Fig. 4. Absorption (a) and emission (b) spectra of HDA-capped ZnS nanoparticles prepared from precursor II at 180°C for 60 min.

distances in the thiourea ligands are typically intermediate between a single and double bond character, which is 1.714 Å. The C–N bond distances range from an intermediate bond character of 1.501 Å to an almost double bond character of 1.344 Å. The S(1)–Zn(1)–Cl(1), Cl(1)–Zn(1)–S(1)1, S(1)1–Zn(1)–Cl(1)1 and S(1)–Zn(1)–Cl(1) bond angles are 105.73°, 110.74°, 105.73° and 112.89°, respectively. The bond angles for two similar ligands, S(1)–Zn(1)–S(1)1 and Cl(1)1–Zn(1)–Cl(1), are 111.33° and 112.68°. These angles deviate from the regular tetrahedral value of 109.47°, which could be explained by the steric interaction between the isopropyl groups.

Synthesis of ZnS nanoparticles

Zinc sulphide (ZnS), a II–VI group semiconductor material, has been extensively investigated due to its immense potential for various device applications.

The band gap of ZnS can be tuned from the ultraviolet to visible region by employing appropriate dopants. It has wide band gaps of 3.5–3.7 eV and 3.7–3.8 eV for zinc blende and wurtzite ZnS, respectively, and can crystallise in two allotropic forms—a cubic form (c-ZnS) with sphalerite structure and a hexagonal form (h-ZnS) with wurtzite structure.

In this study, zinc sulphide nanoparticles were prepared using substituted alkylthiourea complexes, $[ZnCl_2(CS(NHC_6H_{11})_2)_2]$ and $[ZnCl_2(CS(NHC_3H_7)_2)_2]$, as sources of the metal sulphide nanoparticles.

Optical properties of ZnS nanoparticles

The increasing success of the use of alkylthiourea cadmium complexes as single source precursors has led to the investigation of the zinc analogue to prepare ZnS nanoparticles.[27] The band edges for ZnS samples prepared from various methods were blue-shifted in relation to the bulk material (340 nm, 3.64 eV). This is associated with the ZnS nanoparticles being smaller than the bulk exciton of ZnS. There is generally an increase in particle size of nanoparticles with time, which is consistent with an Ostwald ripening process. After an injection of the precursor there is a critical size dependent on the concentration of the precursor. After the depletion of the precursor, the size distribution broadens because the smaller, less stable particles collapse, forming larger particles.

It has recently been reported that nanocrystallites of zinc sulphide doped with manganese have one of the highest photoluminescence efficiencies;[2–5] however, various factors have an influence on the optical properties of nanoparticles, such as the nature of the passivating ligand, temperature and concentration. Therefore, a detailed and thorough understanding of the influence of these factors should be undertaken. The optical properties of the ZnS nanoparticles synthesised from $[ZnCl_2(CS(NHC_6H_{11})_2)_2]$ are shown in Fig. 3. The particles exhibited a band-edge at 278 nm (4.46 eV), a blue shift compared to 340 nm of bulk ZnS. The absorption spectrum showed no visible excitonic features; such bands are prominent in the absorption spectra of CdSe, CdS and ZnSe.

The photoluminescence spectrum showed a broad emission curve with the emission maximum at 318 nm, a red shift in relation to the optical absorption band edge. The position of the band edge of the ZnS nanoparticles prepared from $[ZnCl_2(CS(NHC_3H_7)_2)_2]$ (Fig. 4), is slightly different from that of ZnS from the cyclohexyl complex. The absorption band appears at a slightly higher wavelength (303 nm). The emission spectrum appears narrower with the maximum at 306 nm, a slight red shift in comparison for the band edge. The reduced broadness of the emission peak is probably due to a narrow size distribution.

Structural properties of ZnS nanoparticles

The XRD patterns for the ZnS nanoparticles synthesised from $[ZnCl_2(CS(NHC_6H_{11})_2)_2]$ and $[ZnCl_2(CS(NHC_3H_7)_2)_2]$ are shown in Fig. 5. The diffraction patterns from both samples showed broad peaks typical of nanosized particles. The particles from both complexes showed a mixture of wurtzite and zinc blende zinc sulphide with the wurtzite phase dominant. The predominance of peaks from both complexes (2θ = 23.0°, 29.3° and 41.6°) can be indexed to [002], [102] and [103] of the wurtzite phase. The crystal phases of ZnS are influenced thermodynamically, where higher temperatures favour the wurtzite phase and lower temperatures the cubic sphalerite phase. Therefore the predom-

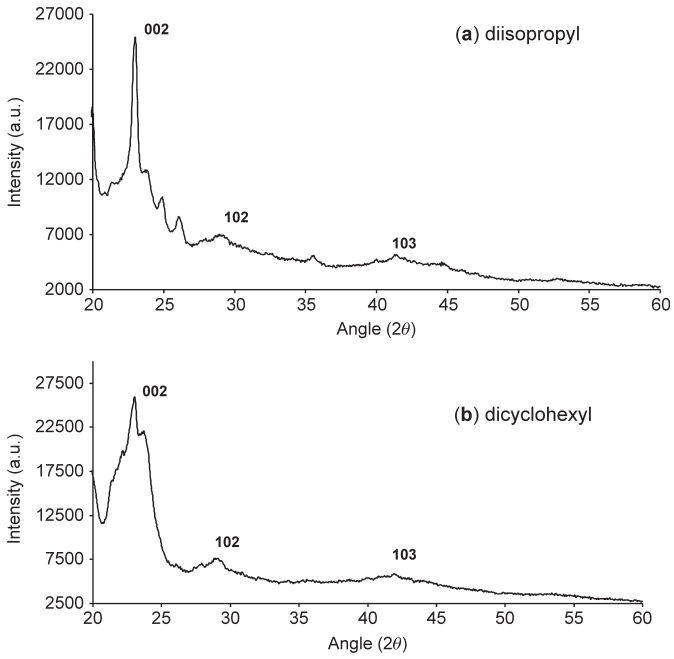

Fig. 5. XRD patterns of ZnS nanoparticles prepared from complexes **II** (**a**) and **I** (**b**).

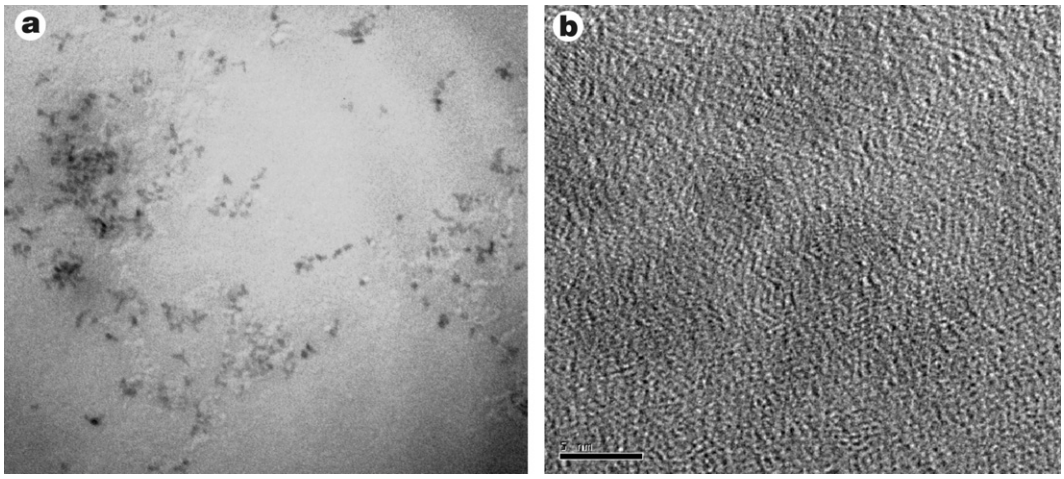

Fig. 6. (**a**) Transmission electron microscopy image of ZnS nanoparticles prepared from precursor I at 180°C. (**b**) High-resolution TEM image of ZnS nanoparticles prepared from precursor I at 180°C.

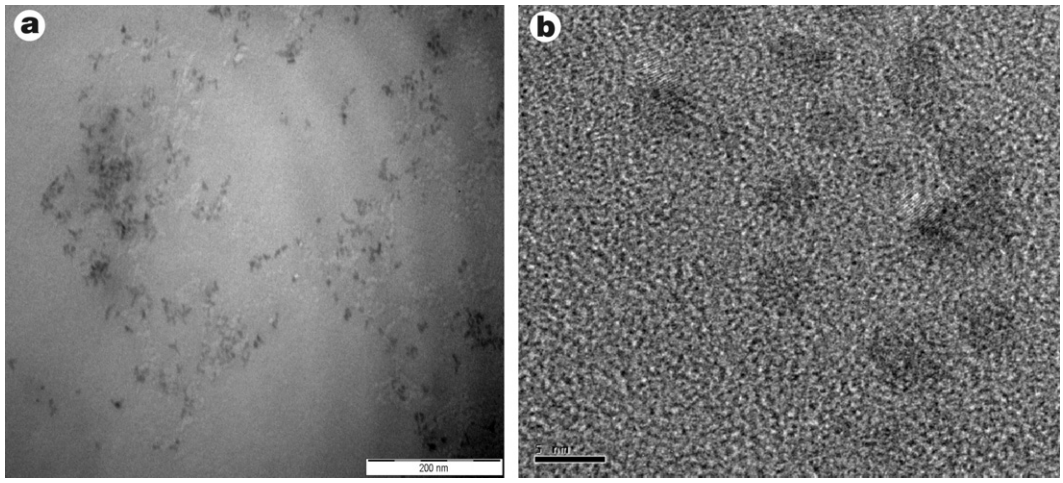

Fig. 7. (**a**) Transmission electron microscopy image of ZnS nanoparticles prepared from precursor II at 180°C. (**b**) High-resolution TEM image of ZnS nanoparticles prepared from precursor II at 180°C.

inance of wurtzite ZnS nanoparticles is possibly due to the high reaction temperature (180°C).

Figures 6 and 7 show the TEM and HRTEM images of the particles synthesised from both precursors. The particles from both samples had a slightly elongated shape with many spherical particles also visible. There was a certain degree of agglomeration and the size of the particles could be approximated to 3–5 nm in diameter. The crystallinity of the nanoparticles was confirmed by the HRTEM images which showed distinct lattice fringes.

Conclusions

The single crystal structures of zinc dicyclohexylthiourea and diisopropylthiourea were obtained. The as-synthesised ZnS nanoparticles resulted in a mixture of elongated and spherical particles of sizes between 3 nm and 5 nm.

This work was supported by the National Research Foundation (South Africa) and Royal Society (United Kingdom).

Received 18 May. Accepted 26 May 2009.

1. Peng W.Q., Qu S.C., Cong G.W., Zhang X.G. and Zhang Z.G. (2005). Optical and magnetic properties of ZnS nanoparticles doped with Mn^{2+}. *J. Cryst. Growth* **282**, 179–185.
2. Bhargava R.N., Gallagher D., Hong X. and Nurmikko A. (1994). Optical properties of manganese-doped nanocrystals of ZnS. *Phys. Rev. Lett.* **72**, 416–419.
3. Sooklal K., Cullum B.S., Angel S.M. and Murphy C.J. (1996). Photophysical properties of ZnS nanoclusters with spatially localized Mn^{2+}. *J. Phys. Chem.* **100**, 4551–4555.
4. Suyver J.F., Wuister S.F., Kelly J.J. and Meijerink A. (2001). Synthesis and photoluminescence of nanocrystalline ZnS:Mn^{2+}. *Nano. Lett.* **1**, 429–433.
5. Dinsmore A.D., Hsu D.S., Gray H.F., Qadri S.B., Tian Y. and Ratna B.R. (1999). Mn-doped ZnS nanoparticles as efficient low-voltage cathodoluminescent phosphors. *Appl. Phys. Lett.* **75**, 802–804.
6. Nicolau Y.F., Dupuy M. and Brunel M. (1990). ZnS, CdS, and $Zn_{1-x}Cd_xS$ thin films deposited by the successive ion layer adsorption and reaction process. *J. Electrochem. Soc.* **137**, 2915–2924.
7. Vacassy R., Scholz S.M., Dutta J., Hofmann H., Plummer C.J.G., Carrot G., Hilborn J. and Akine M. (1998). Nanostructure zinc sulphide phosphors. *Mater. Res. Soc. Symp. Proc.* **501**, 369–374.
8. Calandra P., Goffredi M. and Liveri V.T. (1999). Study of the growth of ZnS in water/AOT/n-Heptane microemulsions by UV absorption spectroscopy. *Colloid Surface Physicochem. Eng. Aspect A* **160**, 9–13.
9. Revaprasadu N., Malik M.A., O'Brien P. and Wakefield G. (1999). Deposition of zinc sulfide quantum dots from a single source molecular precursor. *J. Mater. Res.* **14**, 3237–3240.
10. Ludolph B., Malik M.A., O'Brien P. and Revaprasadu N. (1998). Novel single molecule precursor routes for the direct synthesis of highly monodispersed quantum dots of cadmium or zinc sulfide or selenide. *Chem. Commun.* **17**, 1849–1850.
11. Malik M.A., Revaprasadu N. and O'Brien P. (2001). Air-stable single-source precursors for the synthesis of chalcogenide semiconductor nanoparticles. *Chem. Mater.* **13**, 913–920.
12. Lv R., Cao C.B. and Zhu H.S. (2004). Synthesis and characterization of ZnS nanowires by AOT micelle-template inducing reaction. *Mater. Res. Bull.* **39**, 1517–1524.
13. Heath J.R., Kuekes P.J., Snider G.S. and Williams R.S. (1998). A defect-tolerant computer architecture: opportunities for nanotechnology. *Science* **280**, 1716-1721.

14. Thess A., Lee R., Nikolave P., Dai H., Petit P., Robert J., Xu C.H., Lee Y.H., Kim S.G., Rinzler A.G., Colbert D.T., Scuseria G.E., Tomanek D., Fisher J.E. and Smalley R.E. (1996). Electronic properties of carbon nanotubes probed by magnetic measurements. *Science* **273**, 483-487.
15. Martin C.R. (1994). Nanomaterials: a membrane-based synthetic approach. *Science* **266**, 1961–1966.
16. Martin B.R., Dermody D.J., Reiss B.D., Fang M.M., Lyon L.A., Natan M.J. and Mallouk T.E. (1999). Orthogonal self-assembly on colloidal gold-platinum nanorods. *Adv. Mater.* **11**, 1021–1025.
17. Trentler T.J., Hickman K.M., Goel S.C., Viano A.M., Gibbons P.C. and Buhro W.E. (1995). Solution-liquid-solid growth of crystalline III–V semiconductors: an analogy to vapor–liquid–solid growth. *Science* **270**, 1971–1974.
18. Li Y., Ding Y. and Wang Z. (1999). A novel chemical route to ZnTe semiconductor nanorods. *Adv. Mater.* **11**, 847–850.
19. Hopwood J.D. and Mann S. (1997). Synthesis of barium sulfate nanoparticles and nanofilaments in reverse micelles and microemulsions. *Chem. Mater.* **9**, 1819–1828.
20. Pan Z.W., Dai Z.R. and Wang Z.L. (2001). Nanobelts of semiconducting oxides. *Science* **291**, 1947–1949.
21. Bai Z.G., Yu D.P., Zhang H.Z., Ding Y., Wang Y.P., Gai X.Z., Hang Q.L., Xiong G.C. and Feng S.Q. (1999). Nano-scale GeO_2 wires synthesized by physical evaporation. *Chem. Phys. Lett.* **303**, 311–314.
22. Yang P. and Lieber C.M. (1996). Nanorod-superconductor composites: a pathway to high critical current density materials. *Science* **273**, 1836–1840.
23. Lan C., Hong K., Wang W. and Wang G. (2003). Synthesis of ZnS nanorods by annealing precursor ZnS nanoparticles in NaCl flux. *Solid State Commun.* **125**, 455–458.
24. Trindade T. and O'Brien P. (1996). A single source approach to the synthesis of CdSe nanocrystallites. *Adv. Mater.* **8**, 161–163.
25. Trindade T., O'Brien P. and Zhang M. (1997). Synthesis of CdS and CdSe nanocrystallites using a novel single-molecule precursors approach. *Chem. Mater.* **9**, 523–530.
26. Nair P.S., Revaprasadu N., Radhakrishnan T. and Kolawole G.A. (2001). Preparation of CdS nanoparticles using the cadmium(II) complex of N,N′-bis(thiocarbamoyl)hydrazine as a simple single-source precursor. *J. Mater. Chem.* **11**, 1555–1556.
27. Moloto M.J., Revaprasadu N., O'Brien P. and Malik M.A. (2004). N-alkylthioureacadmium (II) complexes as novel precursors for the synthesis of CdS nanoparticles. *J. Mat. Sci.: Mat. Elec.* **15**, 313–316.
28. Sheldrick G.M. (1997). *SHELXS-97. Program for Crystal Structure Solution.* University of Göttingen, Germany.
29. Burla M.C., Caliandro R., Camalli M., Carrozzini B., Cascarano G.L., De Caro L., Giacovazzo C., Polidori G. and Spagna R. (2005). SIR2004: an improved tool for crystal structure determination and refinement. *J. Appl. Cryst.* **38**, 381–388.
30. Sheldrick G.M. (1997). *SHELXL-97. Program for Crystal Structure Solution.* University of Göttingen, Germany.